Sum-frequency generation in doubly resonant GaP photonic crystal nanocavities

Kelley Rivoire,[1,a)] Ziliang Lin,[1] Fariba Hatami,[2] and Jelena Vučković[1]
[1]*E. L. Ginzton Laboratory, Stanford University, Stanford, California 94305-4085, USA*
[2]*Department of Physics, Humboldt University, D-10115 Berlin, Germany*

(Received 19 April 2010; accepted 2 July 2010; published online 26 July 2010)

We demonstrate and characterize continuous wave $\chi^{(2)}$ sum-frequency generation in gallium phosphide photonic crystal nanocavities. We use two confined modes of the nanocavity in the wavelength range 1500–1600 nm to enhance conversion efficiency. Our results show that these nanocavities can serve as integrated light sources across a range of wavelengths, and are promising for on-chip upconversion of weak intensity telecommunication wavelengths signals to visible wavelengths. © *2010 American Institute of Physics*. [doi:10.1063/1.3469936]

III–V semiconductors such as GaAs and GaP have large second order optical nonlinearities,[1] making them well suited for on-chip nonlinear optical frequency conversion. The poor phase matching due to the cubic symmetry of the zincblende lattice, however, typically limits the conversion efficiency in the absence of quasiphase matching techniques, such as orientation patterning.[2,3] Nanocavities with dimensions smaller than the coherence length of the material[4–6] allow high conversion efficiency, while also minimizing the device footprint. Previously, we showed that small volume (≈cubic optical wavelength in the material) photonic crystal cavities fabricated in GaP, which is transparent at wavelengths longer than 550 nm, can enhance the continuous wave (cw) second harmonic conversion efficiency from infrared to visible light by many orders of magnitude.[7] Here, we demonstrate cw sum-frequency generation (SFG) using two modes of a photonic crystal cavity.

Our structures are fabricated in a 160-nm-thick GaP membrane, which is grown on top of 1 μm $Al_{0.85}Ga_{0.15}P$ on a (100)-oriented GaP wafer by gas-source molecular beam epitaxy. Photonic crystals are defined by e-beam lithography and Cl_2-based dry etching,[8] followed by a hydrofluoric acid undercut of the sacrificial AlGaP layer. The cavity is a modified three-hole linear defect[9] with lattice constant $a=560$ nm, $r/a \approx 0.25$, and slab thickness $d/a \approx 0.3$. We use a perturbation design for our photonic crystal cavities[10] to increase the coupling efficiency between the cavity and objective lens to 5% (verified experimentally by measurements of incident and reflected power). A scanning electron microscope (SEM) image of a fabricated structure is shown in Fig. 1(a). The cavity axes are oriented parallel to the crystal axes.

We characterize the cavity resonances by normal-incidence cross-polarized white light reflectivity, using a tungsten halogen lamp as a source.[8] The cross-polarized configuration is used to obtain sufficient signal-to-noise ratio to observe the Lorentzian resonance above the reflected background uncoupled to the cavity. The white light reflectivity spectrum [Fig. 1(b)] shows several resonant modes (all with transverse-electric polarization), as expected for this cavity design,[11] as well as the electric field intensities for the two modes used in our experiment. Figure 1(c) shows a fit of the fundamental cavity mode to a Lorentzian, giving a quality factor of 3800. A Lorentzian fit of the higher order mode gives a Q of 220. [From finite difference time domain (FDTD) simulations, the expected quality factor of the fundamental mode is 10 000, limited by the thinness of the membrane. The expected quality factor of the higher order mode is 400.] The fundamental mode is primarily polarized along the y-axis [Fig. 1(a)]; the second mode is polarized primarily along the x-axis.

The experimental setup and principle of the experiment are shown in Figs. 2(a) and 2(b). We use two cw lasers, one matched to the wavelength and polarization of the fundamental mode (1565 nm) and one matched to the higher order mode (1504 nm); the nonlinear polarization generates SFG at 767 nm, as well as some second harmonic generation (SHG) at 752 and 782.5 nm. Light from the two lasers is combined on a beamsplitter and passed through an objective lens (NA=0.5) and focused onto the sample; sum frequency and second harmonic signals are collected by the same objective and sent to a spectrometer.

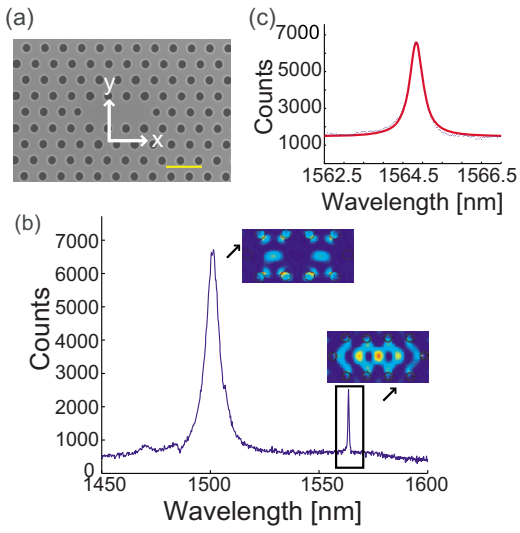

FIG. 1. (Color online) (a) SEM image of a fabricated photonic crystal membrane after undercut of sacrificial layer. Scale bar indicates 1 μm. (b) White light reflectivity from cavity, with FDTD simulations showing electric field of modes of interest. The two modes, both transverse electric-like are polarized orthogonally: the fundamental mode is y-polarized; the higher order mode is x-polarized. (c) Fit to Lorentzian of fundamental mode (peak indicated by black box) with $Q=3800$.

a)Electronic mail: krivoire@stanford.edu.

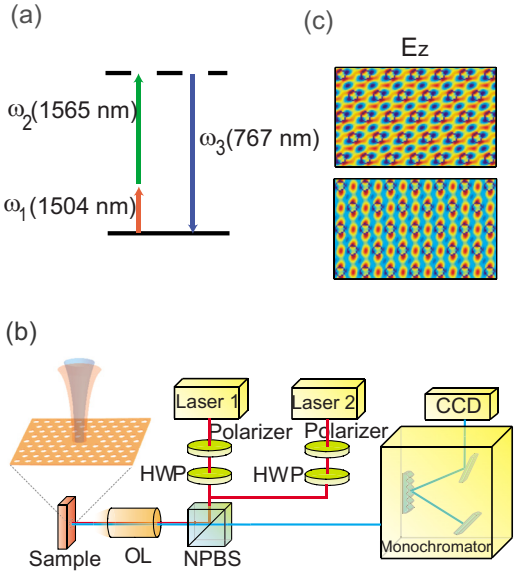

FIG. 2. (Color online) (a) Schematic of SFG process. Incident photons with frequencies ω_1 and ω_2 are converted to frequency ω_3. (b) Experimental setup for SFG. HWP: half wave plate, NPBS: nonpolarizing beamsplitter, and OL: objective lens. The incident light traces the red line into the cavity sample; the sum frequency light follows the blue line into the spectrometer. The polarization of the incident light is controlled by a polarizer and HWP. (c) Simulated electric field pattern of degenerate TM-like Bloch modes of the crystal at wavelength of sum frequency.

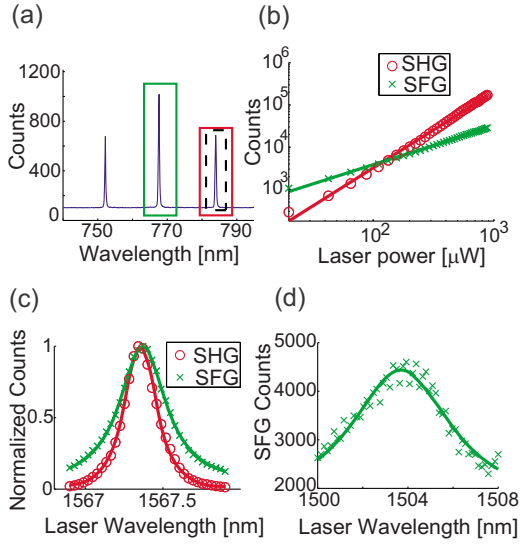

FIG. 3. (Color online) (a) SFG and SHG when two lasers are used to couple into modes shown in Fig. 1. Middle peak (central box) is SFG; right (right and dotted boxes) and left peaks are SHG from each mode. Dotted box indicates second harmonic from fundamental mode over which laser is scanned to measure power and wavelength dependence in (b) and (c). (b) Power dependence of second harmonic and SFG as a function of incident laser power at wavelength of fundamental cavity mode. A polynomial fit plotted on log-log scale gives a coefficient of 0.9 for SFG (×-marks) and 1.8 for second harmonic (circles). The incident power of the second laser at higher order cavity mode wavelength is 6 mW. (c) Wavelength dependence of sum frequency (×-marks) and second harmonic counts (circles) as a function of scanning laser wavelength at fundamental cavity mode. Fit to Lorentzian of SFG counts gives Q of 4300; fit to Lorentzian squared of SHG counts gives Q of 4100, both matching Q of the fundamental mode in Fig. 1, as expected. The other laser is at 1504 nm. (d) Wavelength dependence of sum frequency counts as a function of scanning laser wavelength at higher order cavity mode. Fit to Lorentzian of SFG counts gives Q of 272, matching Q of the higher order mode. Second laser is at 1567.4 nm.

SFG requires field components along x, y, and z axes [since only $\chi^{(2)}_{xyz} \neq 0$ for (100) GaP]. For input beams, we use the two resonant modes of the cavity to provide the x and y oriented components. As in our previous experiments on SHG in these cavities;[7] we use a transverse magnetic-like (TM-like) Bloch mode of the photonic crystal [Fig. 2(c)] with electric field primarily along the z-axis to outcouple SFG light. Phase matching in the cavity geometry requires strong spatial overlap of modes at all three frequencies $P_{\text{out}} \propto P_{\text{in,coupled},1} P_{\text{in,coupled},2} Q_1 Q_2 |\int \chi^{(2)}_{xyz} E_{y,\omega_1} E_{x,\omega_2} E_{z,\omega_3} dV|^2$, where P_{out} is the generated sum frequency radiation, $P_{\text{in,coupled}}$ is the power coupled into the structure at ω_1 or ω_2, and Q_1 and Q_2 are the quality factors of the resonances at ω_1 and ω_2, assuming no depletion of the incident beams. Poor overlap of these three modes limits the measured conversion efficiency $P_{\text{SFG}}/P_{\text{coupled,cavity}}$ to approximately 10^{-8}, where $P_{\text{coupled,cavity}}$ is the coupled laser power in the fundamental mode (coupled power in the higher order mode is an order of magnitude higher).

Figure 3(a) shows a spectrum when both lasers are incident on the cavity; there are three peaks, two due to second harmonic of each laser at the cavity wavelength; the central peak is SFG. We characterize the sum frequency radiation by studying its dependence on the wavelength and power of a single laser, in this case the laser aligned to the fundamental mode of the cavity (black box shows second harmonic from this mode). Figure 3(b) shows the power dependence of SFG counts (sum of counts in green box) and counts from second harmonic at the fundamental wavelength (sum inside red box). A polynomial fit of second harmonic counts shows a power dependence of 1.8, close to the expected 2.0; a fit to the sum frequency counts shows a power dependence of 0.9, close to the expected 1.0. By adjusting the power, we can also control whether we observe more light from SFG or SHG. Figure 3(c) shows the dependence of sum frequency and second harmonic counts (green and red boxes, respectively) on the wavelength of the laser tuned near the fundamental cavity mode. The density of states at the output wavelength is determined by the product of the Lorentzian densities of states for each of the participating input modes $[\rho_c(\lambda) = (Q\lambda/\pi^2 c)(1/1+4Q^2(1-(\lambda/\lambda_c))^2)$ where λ_c and Q are the cavity wavelength and quality factor, respectively, for each mode]. We observe this spectral profile by detuning the laser from the fundamental wavelength of the cavity, while keeping the input beam at the higher order mode fixed. For SHG, we fit the data to a Lorentzian squared, which gives a Q of 4100. For the sum frequency radiation, we fit the data to a Lorentzian, giving a Q of 4300. These Q's are in good agreement with the value measured from cross-polarized reflectivity. To increase the tunable range of the output light, we can alternatively scan the laser at the wavelength of the higher order cavity mode, which has a lower Q [Fig. 3(d)]. Finally, we believe the sum frequency and second harmonic of both cavity modes outcouple through the same TM Bloch mode of the crystal [Fig. 2(c)], as the radiation pattern collected through the objective and imaged onto a camera looks similar at all three wavelengths.

In summary, we have demonstrated cw SFG using two modes of a photonic crystal cavity, which provides a nonlinear optics-based on-chip source that can easily be tuned by changing the frequencies of the cavity resonances. By matching a high Q mode with a low Q mode, we create a source that is tunable over ≈10 nm range. Our structures are prom-

ising for on-chip upconversion of weak infrared signals to visible wavelengths.[12,13] Such a structure could also be used for doubly resonant difference frequency generation, and could be scaled to produce a light source at longer wavelengths (e.g., mid-IR).

Financial support was provided by the National Science Foundation Grant No. DMR-0757112. K.R. and Z.L. are supported by Stanford Graduate Fellowships and the NSF GRFP. This work was performed in part at the Stanford Nanofabrication Facility of NNIN supported by the National Science Foundation under Grant No. ECS-9731293.

[1]I. Shoji, T. Kondo, A. Kitamoto, M. Shirane, and R. Ito, J. Opt. Soc. Am. B **14**, 2268 (1997).
[2]L. A. Eyres, P. J. Tourreau, T. J. Pinguet, C. B. Ebert, J. S. Harris, M. M. Fejer, L. Becouarn, B. Gerard, and E. Lallier, Appl. Phys. Lett. **79**, 904 (2001).
[3]P. S. Kuo, K. L. Vodopyanov, M. M. Fejer, D. M. Simanovskii, X. Yu, J. S. Harris, D. Bliss, and D. Weyburne, Opt. Lett. **31**, 71 (2006).
[4]A. Rodriguez, M. Soljacic, J. D. Joannopoulos, and S. G. Johnson, Opt. Express **15**, 7303 (2007).
[5]M. Liscidini and L. C. Andreani, Appl. Phys. Lett. **85**, 1883 (2004).
[6]M. W. McCutcheon, J. F. Young, G. W. Rieger, D. Dalacu, S. Frédérick, P. J. Poole, and R. L. Williams, Phys. Rev. B **76**, 245104 (2007).
[7]K. Rivoire, Z. Lin, F. Hatami, W. T. Masselink, and J. Vučković, Opt. Express **17**, 22609 (2009).
[8]K. Rivoire, A. Faraon, and J. Vučković, Appl. Phys. Lett. **93**, 063103 (2008).
[9]Y. Akahane, T. Asano, B. Song, and S. Noda, Nature (London) **425**, 944 (2003).
[10]M. Toishi, D. Englund, A. Faraon, and J. Vučković, Opt. Express **17**, 14618 (2009).
[11]A. R. A. Chalcraft, S. Lam, D. O'Brien, T. F. Krauss, M. Sahin, D. Szymanski, D. Sanvitto, R. Oulton, M. S. Skolnick, A. M. Fox, D. M. Whittaker, H. Y. Liu, and M. Hopkinson, Appl. Phys. Lett. **90**, 241117 (2007).
[12]C. Langrock, E. Diamanti, R. V. Roussev, Y. Yamamoto, M. M. Fejer, and H. Takesue, Opt. Lett. **30**, 1725 (2005).
[13]M. A. Albota and F. C. Wong, Opt. Lett. **29**, 1449 (2004).